AN INTELLIGENT CLOUD MONITORING SYSTEM FOR MULTIPLE 3D PRINTERS BASED ON IOT

Yanzhang Xie[1,2], Qingping Yang[1], Wenyi Liu[2], Xizhi Sun[1]*

[1]*Department of Mechanical and Aerospace Engineering, Brunel University London, UK*
[2]*Key Laboratory of Instrumentation Science & Dynamic Measurement, Ministry of Education, North University of China, Taiyuan 030051, China*
** corresponding author: qingping.yang@brunel.ac.uk*

Keywords: 3D PRINTING, IOT (INTERNET OF THINGS), REMOTE MONITORING, LOW-COST SENSORS, CLOUD

Abstract

In the Industry 4.0 era, 3D printing has become a cornerstone of intelligent manufacturing, necessitating precise real-time monitoring and control to ensure efficiency and quality. This research developed an IoT-based cloud monitoring system for 3D printers to enhance remote monitoring and control capabilities. The system collects real-time sensor data on parameters such as temperature and humidity, along with live video feeds. These multimodal data are pre-processed at the edge and further analyzed in the cloud. Users can monitor the 3D printing status via a custom visual interface and adjust parameters based on data analysis to optimize printing quality. To evaluate the system's effectiveness, experiments were conducted to explore the relationship between process parameters and surface roughness and to optimize the printing process and quality using the Taguchi design of experiments. Five factors were considered: nozzle temperature, bed temperature, printing speed, layer height, and ambient temperature. The significant printing process factors were identified, and optimal factor levels were determined to enhance print quality. The experimental results demonstrated that the system can significantly improve the quality and response speed of 3D printing process monitoring. Additionally, it enhances the reliability and user experience of 3D printing.

1. Introduction

In the Industry 4.0 era, intelligent manufacturing drives global transformation, with 3D printing (or additive manufacturing) being one of the core technologies. Fused Deposition Modeling (FDM) is a widely used 3D printing technology due to its design flexibility, efficiency, and cost-effectiveness [1][2]. FDM produces objects through a layer-by-layer accumulation technique using thermoplastic filaments such as PLA, ABS, and PEI [3][4]. Despite its advantages, FDM faces challenges in defect control, including nozzle clogging, heating issues, cooling, vibrations, and environmental changes, which affect print quality and process stability [5][6]. Current 3D printing technology, although advanced, still lacks precise quality control and remote operation capabilities [7].

This research introduces an IoT-based intelligent cloud monitoring system for multiple 3D printers, enabling remote monitoring and optimization through real-time data collection and analysis on a cloud platform. The system's innovative capability lies in its provision of real-time data and video surveillance, the processing and analysis of this data through a combination of edge and cloud computing methodologies, the presentation of salient information via a tailored visual interface, and the optimization of both the printing process and print quality. Users can monitor and adjust printing parameters remotely, achieving higher-quality outputs. Experiments and the Taguchi method are used to explore the relationship between process parameters and surface roughness and to optimize the printing process and quality.

The rest of this paper is organized as follows: Section 2 reviews related work on monitoring 3D printers. Section 3 details the design of the intelligent cloud monitoring system and its components. Section 4 describes the experimental design. Section 5 discusses the experimental results. Section 6 concludes the paper and provides an outlook for future work.

2. Related Work

Existing research on 3D printer quality monitoring focuses on visual observation and physical sensing [8][9]. For instance, Yang et al. used acoustic emission monitoring for filament breakage detection [10], while Kousiatza et al. monitored strain and temperature using fiber Bragg grating sensors [11]. Kakade et al. addressed material flow issues with rotary encoders and load cells [12], and Kwon et al. analyzed the impact of humidity on PLA properties [13].

Visual surveillance methods are also popular. Sánchez et al. used Raspberry Pi for local video monitoring [14], and Liu et al. developed a remote video monitoring system [15]. Nuchitprasitchai and others used webcams for comprehensive local monitoring [16]. However, these methods often lack comprehensive control designs and rely on either physical sensing or visual monitoring, which is not entirely effective.

Recent advancements have made 3D printers more accessible, with the industry experiencing significant growth [17]. Quality monitoring systems are still primarily designed for individual printers, which is insufficient for large-scale networks of 3D printers. To address this, cloud-based remote monitoring systems for multiple 3D printers are essential.

IoT technology connects physical devices to the Internet, enabling intelligent monitoring and management [18]. It has been progressively integrated into 3D printing to enhance monitoring efficiency. Kakade et al. developed an IoT-based real-time monitoring system using Raspberry Pi and sensors [19], while Kazhymurat et al. used embedded sensors and data visualization tools [20]. Our study integrates additional sensors, IoT, and cloud computing to create a smart remote quality monitoring and control system, advancing additive manufacturing towards smart manufacturing [21][22].

3. System Design

3.1 Overall System Design

Traditional 3D printing starts with creating a digital model using CAD, which is then converted into G-code files through slicing software for printing. Users typically need to load these files locally into the 3D printer to start the printing process. Without a remote monitoring system, users must be on-site or within a local network to monitor the printing, limiting mobility and wasting time and resources.

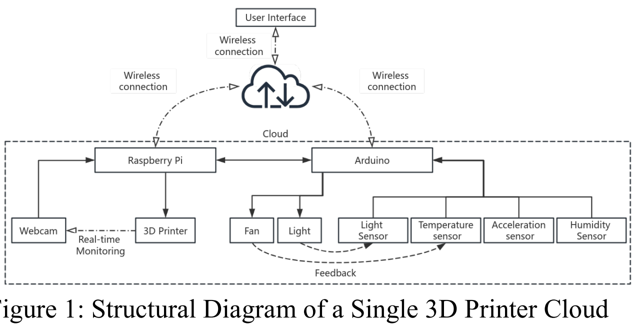

Figure 1: Structural Diagram of a Single 3D Printer Cloud Monitoring System

To address these issues, we integrate IoT with traditional 3D printing technology, developing a system that includes multi-parameter monitoring, video and parameter data fusion, and a visual interface for local and remote monitoring. The system, as shown in Figure 1, is divided into four parts:

Environmental Parameter Monitoring: An Arduino-controlled setup collects environmental data using multiple sensors. The data is pre-processed and sent to the cloud for streaming processing and visualization. The system also includes edge loop feedback control for dynamic adjustment of environmental parameters.

Video Monitoring and 3D Printer Control: A Raspberry Pi with a webcam facilitates real-time video monitoring. The processed video stream is uploaded to the cloud and displayed on a visualization interface. The Raspberry Pi also hosts a compatible operating system to allow remote control of the 3D printer (based on the open-source OctPrint module).

User Interface: A cloud-deployed, user-friendly visualization interface enables bidirectional communication with the cloud. It features multiple sub-interfaces and navigation pages, allowing users to control the printer and adjust environmental parameters remotely.

Cloud: The cloud processes video and sensor data uploaded by the Raspberry Pi and Arduino, displaying it in real-time on the visualization interface. It also receives control commands from the interface to execute instructions via the corresponding microprocessors.

Given the increasing demand for 3D printed products, using a single 3D printer is often insufficient. Therefore, we extend the system to support remote control and monitoring of multiple 3D printers through cloud technology, as shown in Figure 2.

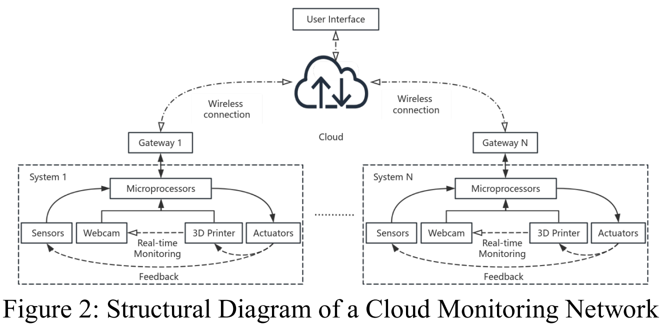

Figure 2: Structural Diagram of a Cloud Monitoring Network System for Multiple 3D Printers

This setup allows users to control multiple monitoring systems via the cloud. To address challenges such as network latency and bandwidth limitations, we incorporate edge computing, which processes data locally before uploading it to the cloud. This approach reduces reliance on the cloud, decreases latency, enhances data security, saves bandwidth and energy, and improves user experience.

3.2 Monitoring of Environmental Parameters

Environmental factors like temperature and humidity significantly impact 3D printing quality. Monitoring these parameters helps optimize printing conditions. We use the

Arduino MKR WIFI 1010 as the main controller, with an Arduino IoT Carrier expansion board integrating various sensors, as shown in Figure 3.

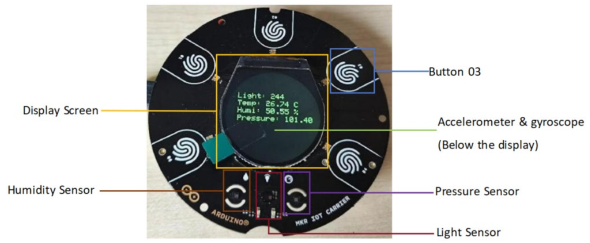

Figure 3: Arduino IoT Carrier Board Mounted Sensors

The monitoring process involves pre-processing sensor data on the Arduino, adjusting environmental conditions if necessary, and sending data to the cloud via MQTT for further processing and visualization. The interface shows real-time environmental data in line charts and dynamic displays, making it user-friendly and intuitive.

3.3 3D Printer Monitoring and Controlling

Relying solely on sensors is not intuitive for users to judge the 3D printing process. Therefore, we set up a video monitoring section using a Raspberry Pi 400 and a USB camera. This setup allows for real-time video monitoring, adjustable for resolution and frame rate based on needs and bandwidth. The Creality Ender-3 printer is controlled locally by connecting it to the Pi, which hosts a control system adapted for the 3D printer, as illustrated in Figure 4. This system establishes a secure bidirectional communication link with the cloud, transmitting video and environmental data for real-time display and enabling remote printer control.

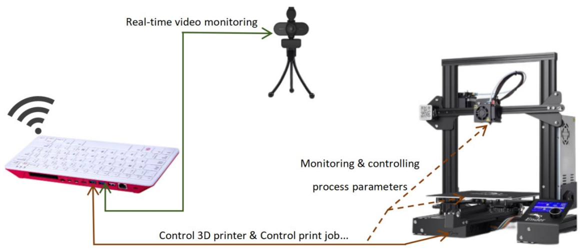

Figure 4: Structural Diagram of the 3D Printer Monitoring System

3.4 Visual User Interface

A comprehensive visual user interface presents monitoring data intuitively, allowing users to understand and control the 3D printing process easily. Our cloud-based web interface is accessible anywhere with Internet access and includes a secure login. The main interface displays sensor data in real-time graphs and numerical values. The 3D printer control interface is accessible via a navigation pop-up window to prevent accidental navigation, as shown in Figure 5.

Figure 5: Main Interface and Navigation Pop-up Window

The cloud control interface for 3D printers features preview windows for multiple printers and a multifunctional control panel (based on OctoEverywhere), as shown in Figure 6.

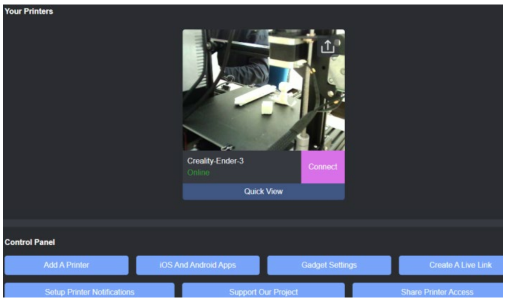

Figure 6: Cloud Control Interface for 3D Printers

The local control main interface (based on OctoPrint) includes areas for manipulating G-code files, monitoring and controlling print tasks, and displaying additional printing information, as detailed in Figure 7.

3.5 Cloud

Figure 8 outlines a three-layered system architecture comprising the Local, Cloud, and Application Layers. The Local Layer leverages Arduino boards for environmental monitoring and 3D printer control, using MQTT protocols and encrypted channels for secure data transmission. The Cloud Layer constitutes the central component of the system, encompassing stream analytics, data storage, a web application, an IoT Hub facilitating seamless device-to-cloud interactions, and a proxy server to bolster security measures. In addition, machine learning-based modules including fault prediction, auto-adjustment and quality optimization are deployed in this layer, significantly boosting system reliability and operational efficiency. The Application layer has a cloud-hosted interface that can visualize all data results.

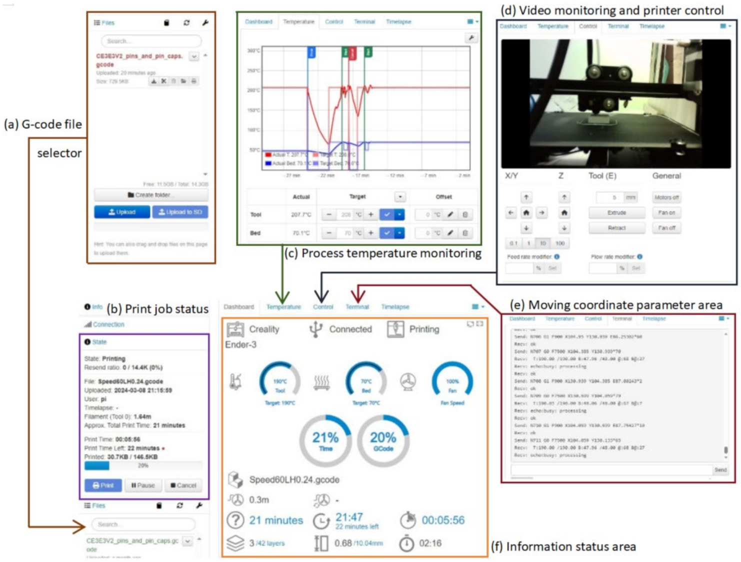

Figure 7: Local Control Main Interface and Sub-interfaces of the 3D Printer

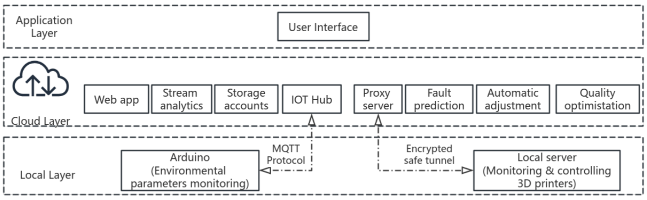

Figure 8: System Layer Diagram

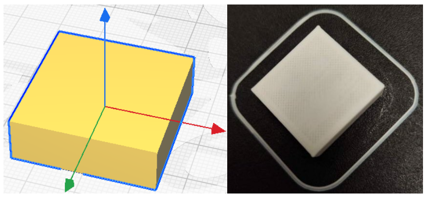

Figure 9 Test sample model and Test sample entity

3.6 Alarms and Notifications

The system features a local alarm, activated by a buzzer, and employs algorithms for environmental monitoring to detect anomalies. Upon detection, it displays notifications on the user interface and allows users to customize how they receive alerts, including options for emails and text messages. This customization aids in keeping users informed about environmental issues and the status of monitoring tasks.

4. Experiments

The developed system facilitates continuous monitoring, data storage, and dynamic control, enabling an in-depth study of the system's capacity to optimize 3D printing processes. To evaluate the system's effectiveness, we conducted experiments to explore the relationship between process parameters and surface roughness, and optimize the printing process and quality using the Taguchi design of experiment.

4.1 Specimen Preparation

In the experiments, the test samples were designed as rectangular PLA prisms with dimensions of 30 × 30 × 10 mm. The model's infill density was set at 20%, with a cubic infill structure. The test sample model and the actual test sample are shown in Figure 9.

In the experiments, a surface roughness tester was used to measure the roughness of the top and bottom surfaces of the test samples. On each surface, the roughness at 5 different positions was measured, as shown in Figure 10. The surface average roughness at these positions is represented as Ra_1, Ra_2, Ra_3, Ra_4 and Ra_5.

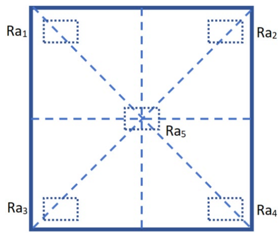

Figure 10 Test Sample Measurement Position (Top View)

4.2 Design of Experiments

This study utilized the Taguchi method for experimental design, focusing on five factors: ambient temperature, nozzle temperature, bed temperature, printing speed, and layer height. The ambient temperature is set at two levels, whereas the other factors are at three levels. The selected values for these factors are aligned with the optimal parameter range for PLA material. An L18 orthogonal array was used to plan the experimental runs, as shown in Tables 1 and 2.

Table 1 Experimental factor parameters and their levels

Factor	Code	Level		
		1	2	3
Environmental Temperature	A	19℃	29℃	/
Nozzle Temperature	B	190℃	208℃	225℃
Print bed Temperature	C	25℃	48℃	70℃
Print Speed	D	30 mm/s	60 mm/s	90 mm/s
Layer Height	E	0.12 mm	0.24 mm	0.36 mm

4.3 Measurement of surface roughness

The surface roughness of the specimens was measured using a MarSurf PS 10 surface roughness tester from Mahr. The probe was moved across the surface of each specimen to obtain the roughness Ra value, which was displayed on the device's screen and recorded for analysis. A leveled square iron block served as a support platform to ensure the accurate positioning of the specimens during measurement.

Table 2 L18 Experimental Factorial Orthogonal Array

Order	Control factors				
	A(℃)	B (℃)	C(℃)	D(mm/s)	E(mm)
1	19	190	25	30	0.12
2	19	190	48	60	0.24
3	19	190	70	90	0.36
4	19	208	25	30	0.24
5	19	208	48	60	0.36
6	19	208	70	90	0.12
7	19	225	25	60	0.12
8	19	225	48	90	0.24
9	19	225	70	30	0.36
10	29	190	25	90	0.36
11	29	190	48	30	0.12
12	29	190	70	60	0.24
13	29	208	25	60	0.36
14	29	208	48	90	0.12
15	29	208	70	30	0.24
16	29	225	25	90	0.24
17	29	225	48	30	0.36
18	29	225	70	60	0.12

5. Results and discussions

5.1 Measurement results

Table 3 presents the surface roughness measurements for the top surfaces of the test samples, indicating variability in the outcomes. Experiment run 11 exhibited the highest average surface roughness at 4.1996 μm, suggesting a coarser surface, while Experiment run 8 had the lowest at 1.4522 μm, indicative of a smoother surface. These results highlight the impact of the varied printing parameters on surface roughness.

Table 3 Top surface roughness measurement results

Sample	Ra_1	Ra_2	Ra_3	Ra_4	Ra_5	Average
1	3.196	3.560	1.577	3.217	3.494	3.0088
2	3.744	4.059	2.700	2.467	2.812	3.1564
3	2.305	3.826	3.950	2.687	3.119	3.1774
4	1.091	1.552	2.399	3.599	1.561	2.0404
5	2.527	1.912	2.611	2.808	1.802	2.3320
6	3.228	3.180	3.922	3.219	3.047	3.3192
7	2.978	2.572	3.096	3.044	2.258	2.7896
8	1.879	2.012	1.043	0.781	1.546	1.4522
9	2.440	2.096	1.888	1.818	2.638	2.1760
10	2.752	3.868	2.684	2.901	2.933	3.0276
11	4.078	3.863	3.488	4.242	5.327	4.1996
12	4.091	3.286	3.409	3.480	3.954	3.6440
13	2.980	2.504	2.816	2.727	2.621	2.7296
14	2.634	3.424	3.645	3.295	3.221	3.2438
15	3.510	3.879	2.643	3.971	4.065	3.6136
16	2.256	2.799	3.411	2.934	3.151	2.9102
17	2.821	3.178	1.690	2.518	3.488	2.7390
18	2.792	4.084	3.608	3.296	3.963	3.5486

Unit: μm

Table 4 reports the surface roughness measurements for the bottom surfaces of the test samples, revealing significant variations. The highest average roughness was observed in Run 12 at 5.1298 μm, whereas Run 16 exhibited the lowest at 3.3282 μm.

Table 4 Bottom surface roughness measurement results

Sample	Ra1	Ra2	Ra3	Ra4	Ra5	Average
1	4.986	4.174	4.030	3.480	4.258	4.1856
2	4.165	3.826	4.436	4.927	4.344	4.3396
3	4.396	4.590	4.455	3.795	4.974	4.4420
4	2.769	3.082	3.900	4.157	4.162	3.6140
5	4.389	3.228	4.175	3.753	4.545	4.0180
6	3.227	4.128	3.996	3.910	4.377	3.9276
7	3.352	3.034	4.347	3.237	3.693	3.5326
8	3.431	3.179	4.010	3.733	3.403	3.5512
9	2.747	3.197	4.448	4.293	3.288	3.5946
10	4.742	3.435	3.062	3.956	3.888	3.8166
11	4.638	3.970	5.019	4.521	4.395	4.5086
12	5.188	5.249	4.050	5.797	5.365	5.1298
13	5.264	4.039	4.558	3.890	5.301	4.6104
14	3.895	4.403	4.601	4.770	4.385	4.4108
15	4.292	4.443	4.866	3.431	3.741	4.1546
16	3.819	3.790	3.380	3.291	2.361	3.3282
17	3.367	3.635	3.768	4.223	2.432	3.4850
18	4.583	5.021	4.818	4.289	3.254	4.3930

Unit: μm

5.2 Optimization of process parameters

Table 5 illustrates the analysis of means for top surface roughness of the printed samples, using Delta and Rank to evaluate the influence of different parameters. The data indicates that nozzle temperature (Factor B), with the highest Delta value of 0.766, has the most significant impact on surface roughness, followed by ambient temperature (Factor A) and layer height (Factor E). These factors are ranked accordingly, emphasizing their importance in the optimization of 3D printing settings.

Table 5 Means Response Table for Top Surface Roughness

Level	A	B	C	D	E
1	2.606	3.369	2.751	2.963	3.352
2	3.295	2.880	2.854	3.033	2.803
3	/	2.603	3.246	2.855	2.697
Delta	0.689	0.766	0.495	0.178	0.655
Rank	2	1	4	5	3

Figure 11 and Table 5 together inform the optimal printing parameters for reducing surface roughness on the top surfaces of printed samples. The best results were observed at an ambient temperature of 19°C, nozzle temperature of 225°C, print bed temperature of 25°C, print speed of 90 mm/s, and layer height of 0.36 mm. Notably, the nozzle temperature demonstrates a pronounced impact on surface roughness, as evidenced by its significant fluctuations in the main effects plot.

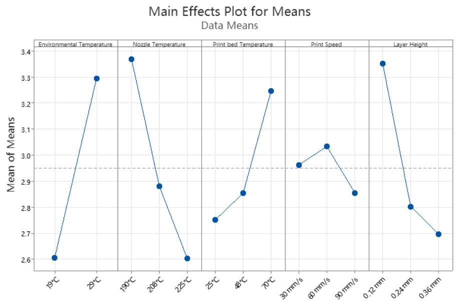

Figure 11 Main effects plot of Means for Top Surface Roughness

Table 6 summarizes the analysis of means for bottom surface roughness of printed samples. Nozzle temperature has the most significant impact on roughness (Delta=0.756), followed by print bed temperature and print speed.

Table 6 Means Response Table for Bottom Surface Roughness

Level	A	B	C	D	E
1	3.912	4.404	3.848	3.924	4.160
2	4.204	4.123	4.052	4.337	4.020
3		3.647	4.274	3.913	3.994
Delta	0.292	0.756	0.426	0.425	0.165
Rank	4	1	2	3	5

Figure 12 and Table 6 together determine the optimal parameters for minimizing bottom surface roughness in 3D printing. The optimal settings are an ambient temperature of 19°C, nozzle temperature of 225°C, print bed temperature of 25°C, printing speed of 90 mm/s, and layer height of 0.36 mm. The results highlight the pronounced effect of nozzle temperature on surface roughness.

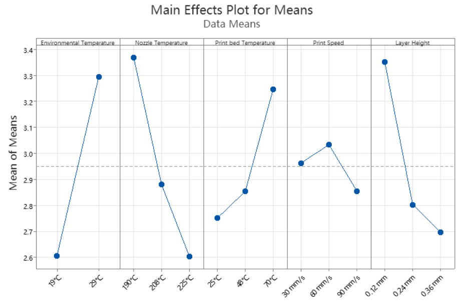

Figure 12 Main effects plot of Means for Bottom Surface Roughness

5.3 Analysis of variance (ANOVA)

According to the ANOVA presented in Table 7, the relative impact of various factors on the surface roughness of 3D printed samples can be determined.

The ANOVA results for top surface roughness indicate that ambient temperature has the most significant effect, contributing 29.13% to the variance, while printing speed has the least impact at only 1.32%. Ambient temperature, nozzle temperature, and layer height are statistically significant factors ($p < 0.05$) affecting top surface roughness.

The significant influence of ambient temperature is likely due to its effect on the cooling rate of the extruded material. To maintain a stable ambient temperature of 19°C, windows and doors were opened, leading to potential air drafts or breezes, which could have introduced variability in the cooling rate, thereby affecting surface roughness.

Additionally, within a certain range, an increase in nozzle temperature results in a decrease in surface roughness. This is because higher nozzle temperatures make the extruded PLA material softer and easier to shape, resulting in smoother surfaces. Conversely, lower nozzle temperatures reduce printing precision, thereby increasing roughness.

Table 7 Analysis of variance (ANOVA) for the Mean of Top Surface Roughness

Source	DF	Seq SS	Contribution(%)	Adj MS	F	P
A	1	2.13831	29.13	2.13831	17.17	0.003
B	2	1.80691	24.62	0.90346	7.26	0.016
C	2	0.82037	11.18	0.41018	3.29	0.090
D	2	0.09677	1.32	0.04838	0.39	0.690
E	2	1.48196	20.19	0.74098	5.95	0.026
Residual Error	8	0.99611	13.57	0.12451		
Total	17	7.34042				

Table 8 shows the ANOVA results for bottom surface roughness, highlighting nozzle temperature as the predominant factor, contributing 43.53% to roughness variability. Notably, ambient temperature and print speed are also significant factors. In contrast, layer height contributes minimally, at only 2.36%.

Table 8 Analysis of variance (ANOVA) for the Mean of Bottom Surface Roughness

Source	DF	Seq SS	Contribution(%)	Adj MS	F	P
A	1	0.38480	9.55	0.38480	5.61	0.045
B	2	1.75345	43.53	0.87673	12.78	0.003
C	2	0.54395	13.50	0.27198	3.97	0.064
D	2	0.70261	17.44	0.35130	5.12	0.037
E	2	0.09516	2.36	0.04758	0.69	0.527
Residual Error	8	0.54861	13.62	0.06858		
Total	17	4.02858				

The analysis underscores that due to the bottom surface's proximity to the heated print bed, ambient temperature's influence is mitigated. This study confirms the overriding impact of nozzle temperature on the bottom surface's quality, emphasizing its importance in optimizing 3D print quality.

5.4 Linear regression

In this study, linear regression analysis quantifies the impact of process parameters on surface roughness, with each regression model including a 95% confidence interval. The significance threshold for these models is set at $p < 0.05$. The regression equations are:

$$\text{TopSurfaceRoughness} = 6.09 + 0.0689 \times \text{Environmental Temperature} - 0.02195 \times \text{Nozzle Temperature} + 0.01096 \times \text{Print Bed Temperature} - 0.00180 \times \text{Print Speed} - 2.728 \times \text{Layer Height} \quad (1)$$

$$\text{BottomSurfaceRoughness} = 7.56 + 0.0292 \times \text{Environmental Temperature} - 0.02155 \times \text{Nozzle Temperature} + 0.00946 \times \text{Print Bed Temperature} - 0.00018 \times \text{Print Speed} - 0.689 \times \text{Layer Height} \quad (2)$$

Table 9 provides the R-squared values, indicating the proportion of variance each model explains for the respective surface roughness. The top surface model has an R^2 of 81.19%, demonstrating a strong correlation between the parameters and the surface roughness, hence showing high predictive power. For the bottom surface, the R^2 of 67.45% suggests that while the relationship is significant, and it captures a lower proportion of the variance compared to the top surface.

Residual plots, as illustrated in Figure 13, are essential for assessing the fit of regression models. The normal probability plots show residuals closely aligning with a straight line, indicative of normal distribution. This observation is supported by the histograms, which exhibit symmetry around zero, suggesting the normality of the residuals. Additionally, the scatter plots of residuals versus fitted values and versus order show randomness without discernible patterns or trends, confirming constant variance and unbiased data collection. These plots demonstrate that the models adequately capture the dynamics of the process.

Table 9 Model Summary

	S	R-sq	R-sq (adj)	R-sq (pred)
Top Surface	0.339217	81.19%	73.35%	59.14%
Bottom Surface	0.330562	67.45%	53.89%	25.93%

The optimum process parameters obtained in the Taguchi experimental design can be implemented in the remote control of the 3D printers to optimize the print quality, which can be also predicted using the regression models.

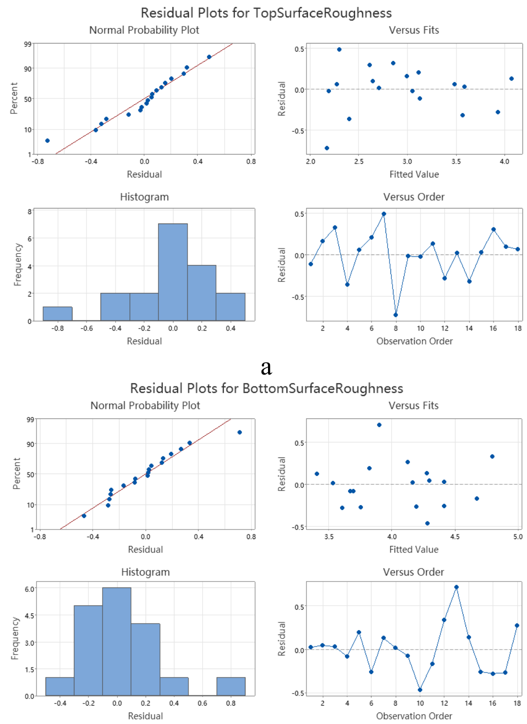

Figure 13 (a) Residual plots for top surface roughness (b) Residual plots for top surface roughness.

6. Conclusions

In In the era of Industry 4.0, 3D printing has become pivotal to intelligent manufacturing. This study introduces an IoT-based smart 3D printer cloud monitoring system to address the challenges of limited monitoring and inadequate remote quality control inherent in traditional 3D printing. The system integrates environmental parameter collection, real-time video, edge pre-processing, and cloud-based analysis, thereby enhancing the timeliness and accuracy of 3D printing monitoring and improving print quality.

A key innovation of the system is its ability to process multi-source heterogeneous data and effectively coordinate edge and cloud computing. It features a real-time, user-friendly monitoring interface and a custom-designed visual UI that simplifies operations, allowing for easy remote adjustments and parameter optimization. The effectiveness of this system in improving 3D printing results was validated using a print quality optimization experiment based on the Taguchi method.

Experiments investigated the process parameters through the cloud monitoring system to study their impact on surface roughness. The system enabled continuous remote monitoring, cloud data storage and analysis, and dynamic control, markedly enhancing the quality and response speed of the 3D printing process. The user-friendly interface and real-time data analysis significantly improved reliability and user experience, allowing for precise adjustments based on immediate feedback and comprehensive oversight of printing operations, thus optimizing outcomes and operational efficiency.

However, the study acknowledges limitations, such as its dependency on specific environmental parameters and material choices, and limited verification across a broader range of conditions. Future research will focus on augmenting data analysis through the integration of machine learning and artificial intelligence to enable fault prediction, automatic adjustment, and quality optimization. Additionally, efforts will be directed toward expanding the system's versatility to accommodate a range of materials and parameters, enhancing system security and stability to ensure robust performance in intricate industrial settings, and refining the user interface for greater intuitiveness and expedited response times.

In conclusion, this study presents an innovative approach to leveraging 3D printing technology in intelligent manufacturing, advancing remote real-time quality monitoring and control capabilities with wide applications.

References:

[1] Berman, B.:‘3-D printing: The new industrial revolution’, Bus. Horiz., 2012, 55, (2), pp. 155-162.

[2] Bräuer, G., Sachsenhofer, K., and Lang, R.W.:‘Material and process engineering aspects to improve the quality of the bonding layer in a laser-assisted fused filament fabrication process’, Additive Manufacturing, 2021, 46, pp. 102105.

[3] Lee, J., An, J., and Chua, C.K.:‘Fundamentals and applications of 3D printing for novel materials’, Applied Materials Today, 2017, 7, pp. 120-133.

[4] Picard, M., Mohanty, A.K., and Misra, M.:‘Recent advances in additive manufacturing of engineering thermoplastics: challenges and opportunities’, RSC Advances, 2020, 10, (59), pp. 36058-36089.

[5] Shen, Z., Shang, X., Zhao, M., et al.:‘A learning-based framework for error compensation in 3D printing’, IEEE Transactions on Cybernetics, 2019, 49, (11), pp. 4042-4050.

[6] Jin, Y., Du, J., He, Y. and Fu, G.:‘Modeling and process planning for curved layer fused deposition’, The International Journal of Advanced Manufacturing Technology, 2017, 91, pp. 273-285.

[7] Jiang, S., Siyajeu, Y., Shi, Y., et al.:‘Improving the forming quality of fused filament fabrication parts by applied vibration’, Rapid Prototyping Journal, 2019, 26, (1), pp. 202-212.

[8] Kantaros, A. and Karalekas, D.:‘Fiber Bragg grating based investigation of residual strains in ABS parts fabricated by fused deposition modeling process’, Mater Des, 2013, 50, pp. 44-50.

[9] Kantaros, A., Giannatsis, J. and Karalekas, D.:‘A novel strategy for the incorporation of optical sensors in Fused Deposition Modeling parts’, Proc. Int. Conf. Adv. Manuf. Eng. Technol., Stockolm, Sweden, 2013, pp. 163-170.

[10] Yang, Z., Jin, L., Yan, Y. et al.:‘Filament breakage monitoring in fused deposition modeling using acoustic emission technique’, Sensors, 2018, 18, (3), pp. 749.

[11] Kousiatza, C. and Karalekas, D.:‘In-situ monitoring of strain and temperature distributions during fused deposition modeling process’, Mater Des, 2016, 97, pp. 400-406.

[12] Kakade, S., Mulay, A. and Patil, S.:‘IoT-based real-time online monitoring system for open ware FDM printers’, Materials Today: Proceedings, 2022, 67, pp. 363-367.

[13] Kwon, S., Lee, S., Kim, Y., et al.:‘A filament supply system capable of remote monitoring and automatic humidity control for 3D printer’, Journal of Sensors, 2020, 2020, (1), pp. 1-10.

[14] Sanchez, G.A.G., Vaca, A.R., Manzano, S. et al.:‘Print server with web user interface for real-time image control and monitoring of a 3D printer using open source tools’, CISTI, 2017, pp. 1-4.

[15] Liu, C., Jiang, P. and Jiang, W.:‘Embedded-web-based remote control for RepRap-based open-source 3D printers’, IECON 2017 - 43rd Annual Conference of the IEEE Industrial Electronics Society, 2017, pp. 3384-3389.

[16] Nuchitprasitchai, S., Roggemann, M.C. and Pearce, J.M.:‘Three hundred and sixty degree real-time monitoring of 3-D printing using computer analysis of two camera views’, Journal of Manufacturing and Materials Processing, 2017, 1, (1), pp. 2.

[17] Wohlers, T., Campbell, R.I., Diegel, O., et al.:‘Wohlers Report 2020 3D Printing and Additive Manufacturing State of the Industry’, 2020.
[18] Singh, R., Gehlot, A., Akram, S.V., et al.:‘Cloud manufacturing, internet of things-assisted manufacturing and 3D printing technology: reliable tools for sustainable construction’, Sustainability, 2022, 13, (13), pp. 7327.
[19] Kakade, S., Mulay, A. and Patil, S.:‘IoT-based real-time online monitoring system for open ware FDM printers’, Materials Today: Proceedings, 2022, 67, pp. 363-367.
[20] Kazhymurat, T., Shehab, E. and Ali, M.H.:‘IoT-based real-time 3D printing monitoring system," 2022, SIST, pp. 1-5.
[21] Wu, D. , Liu, X., Hebert, S., et al.:‘Democratizing digital design and manufacturing using high performance cloud computing: Performance evaluation and benchmarking’, Journal of Manufacturing Systems, 2017, 43, pp. 316-326.
[22] Wang, L., Törngren, M. and Onori, M.:‘Current status and advancement of cyber-physical systems in manufacturing’, Journal of Manufacturing Systems, 2015, 37, pp. 517-527.